HAL open science

Active jamming of microswimmers at a bottleneck constriction

Edouardo Al Alam, Marvin Brun-Cosme-Bruny, Vincent Borne, Sylvain Faure, Bertrand Maury, Philippe Peyla, Salima Rafaï

To cite this version:

Edouardo Al Alam, Marvin Brun-Cosme-Bruny, Vincent Borne, Sylvain Faure, Bertrand Maury, et al.. Active jamming of microswimmers at a bottleneck constriction. Physical Review Fluids, 2022, 7 (9), pp.L092301. 10.1103/PhysRevFluids.7.L092301 . hal-03790442

HAL Id: hal-03790442

https://hal.science/hal-03790442v1

Submitted on 28 Sep 2022

HAL is a multi-disciplinary open access archive for the deposit and dissemination of scientific research documents, whether they are published or not. The documents may come from teaching and research institutions in France or abroad, or from public or private research centers.

L'archive ouverte pluridisciplinaire **HAL**, est destinée au dépôt et à la diffusion de documents scientifiques de niveau recherche, publiés ou non, émanant des établissements d'enseignement et de recherche français ou étrangers, des laboratoires publics ou privés.

Active jamming of microswimmers at a bottleneck constriction

Edouardo Al Alam, Marvin Brun-Cosme-Bruny, Vincent Borne, Philippe Peyla, and Salima Rafaï
Univ. Grenoble Alpes, CNRS, LIPhy, F-38000 Grenoble, France

Sylvain Faure
Laboratoire de Mathématiques d'Orsay, Université Paris-Saclay, 91405 Orsay Cedex, France

Bertrand Maury
Département de Mathématiques Appliquées, Ecole Normale Supérieure, Université PSL, Paris, France and Laboratoire de Mathématiques d'Orsay, Université Paris-Saclay, 91405 Orsay Cedex, France
(Dated: September 16, 2022)

When attracted by a stimulus (light), microswimmers can build up very densely at a constriction and thus cause jamming. The micro-alga *Chlamydomonas Reinhardtii* is used here as a model system to study this phenomenon. Its negative phototaxis makes the algae swim away from a light source and go through a microfabricated bottleneck-shaped constriction. Successive jamming events interspersed with bursts of algae are observed. A power law decrease describes well the distribution of time lapses of blockages. Moreover, the evacuation time is found to increase when increasing the swimming velocity. These results are reminiscent of crowd dynamics and in particular what has been called the Faster is Slower effect in the dedicated literature. It also raises the question of the presence of tangential solid friction between motile cells densely packed. Furthermore, we demonstrate the existence of a transition from a jammed phase described by a power law decrease to an uninterrupted phase described by an exponential decay, we characterize such a transition as a function of door size and swimming velocity. Interestingly, the exponential flowing regime shows what might be referred to as 'a faster is faster' regime.

In bio-technologies, harvesting micro-organisms such as bacteria [1] or micro-algae [2] is now a tremendous challenge to extract new drugs and chemicals [3, 4]. Several microfluidic devices have recently emerged to achieve such a task [5–7]. A jamming phase can often occur when concentrated cells are transported by a fluid [8–10]. At the micro-scale, jamming results from the accumulation of cells at a constriction, leading to the build-up of fouling layers. Jamming can severely disrupt the performance of microfluidic devices [11]. Initially, it reduces the permeability of channels or pores and eventually leads to a complete obstruction of the flow [12, 13]. Jamming is thus one of the leading causes of efficiency loss in high-throughput technologies processes [14]. To remedy fouling and jamming, it is usually necessary to completely stop the process and use cleaning strategies that consume energy and time before restarting the process [15]. Motile cells (bacteria or micro-algae) can self-accumulate without an external flow and can go to nest in a particular place of the circuit (pores, porous regions, constrictions) thus forming an active jamming that is essential to characterize. Beyond jamming, this type of accumulation can be a precursor to formation of bio-films.

More generally, jamming problems occur in extremely varied situations that are nowadays very much studied in the context of crowd dynamics. Crowd motion modeling has become a very active field of research, and serious debates on how to model certain behaviors such as panic movements are still ongoing in the community [16]. In this particular case, the Faster is Slower (FiS) effect plays a central role: it essentially indicates that, in certain situations where the crowd is very dense, the willingness of individuals is to increase their speed when making an effort to evacuate, which has the effect of blocking the entire evacuation process. In addition, it has been established that these paradoxical effects observed in crowd dynamics persist in a very wide variety of systems: in a granular silo [17], in a suspension [18] as well as in a flock of sheep or in a crowd of pedestrians [19]. A physicist's approach is us to look for a common physical mechanism behind these observable measured values. At a minimum, it would be desirable to succeed in defining universality classes in this family of problems. In particular, a class of systems could be that of active suspensions. In this work, we introduce active suspensions as a class of crowds and focus our study on jamming events occurring at a constriction due to cell build-up of microalgae. Understanding behavior of highly concentrated motile micro-organisms and especially their short-range interactions through adhesion or friction remains a challenge. In our experiments, we use a negative phototactic strain of green algae *Chlamydomonas Reinhardtii* (CR) swimming away from light and moving toward a constriction (Fig. 1b). We iden-

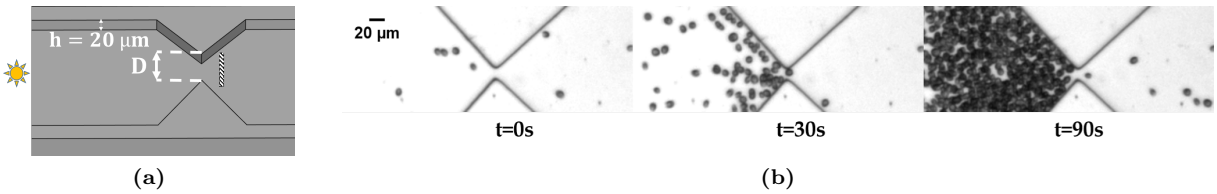

(a) (b)

FIG. 1: a) Schematic of bottleneck shaped micro-channel of thickness 20 µm $\sim 2\times$diameter of CR. The dashed rectangle represents the zone over which time lapses are measured. A light source is placed on the left, triggering a left to right swimming motion. b) Snapshots of the jamming process through a $D = 10$ µm constriction at different times.

tify jamming events and analyze the dynamics of evacuation. The greater the velocity of the algae, the greater the active jamming. This phenomenon is very similar to the FiS effect mentioned above.

Experimental details

CR is a bi-flagellate photosynthetic cell [20] with diameter $a = 10$ µm . Cells are grown under a 14h/10h light/dark cycle at 22°C in TAP medium (Tris Acetate Phosphate) and are harvested in the middle of the exponential growth phase. CR's front flagella beat in a breaststroke manner and propel the cell in the fluid. The swimming is characterized by a persistent random walk in absence of bias [21, 22]. However, in the presence of a light stimulus (green wavelength, i.e., around 510 nm), the strain used in this study (CC-124) tends to swim away from the light source and perform a ballistic motion [23], this is known as negative phototaxis. CR suspension is concentrated by centrifuging 40 mL at 1000 rpm for 15 min and removing the supernatant, the solution is then placed under a red light for 2h. Velocity is controlled by increasing the medium's viscosity via Dextran addition [24, 25]. Cells are finally introduced within a microfluidic device composed of two reservoir chambers of height 20 µm (twice the cell diameter) linked by a bottleneck constriction of varying width $D = 10, 20, 30, 50$ µm (Fig.1a). Microfabrication is made of transparent PDMS by means of soft lithography processes [26], BSA (Bovine serum albumin) is used to passivate the device and avoid cells' adhesion.

We observe the cells under a bright field inverted microscope (Olympus IX71, magnification x4) coupled to a 14 bit CCD camera (Prosilica GX) used at a framerate of 20 fps. The sample is enclosed in a black box with two red filtered windows for visualization in order to prevent the microscope light from triggering phototaxis.

The algae are initially distributed homogeneously in the chamber. A white LED light is switched on the left side of the sample. Negative phototaxis makes the microswimmers swim toward walls and at the constriction. Particle tracking is performed using the library Trackpy [27, 28]. The volume fraction of cells when very dense regimes are reached is deduced from grey level intensity measurements that were calibrated beforehand. Fig.1b illustrates one typical geometry of the experiments. The sequence shows a series of microscopy images at different timescales following the light stimulus. The microswimmers swim away from the light and toward the constriction (from left to right). The sampling window is located on the right hand side (downstream) at 40 µm from the constriction with a width of 1.375 µm (1 px) and a height chosen as 1.5 times the diameter D (Fig.1a). Analyses are done after a stable build-up is formed at the door with a volume fraction $\phi \approx 55$ % to avoid any effect of density variation. Critical clogging (*i.e.* permanently clogged door) was never observed during our experiments. A stationary state characterized by a constant volume fraction at the constriction and cells exiting the constriction is observed along the whole duration of an experiment. However, experiments can not be carried out on a duration exceeding 40 min as cells are observed to lose their sensitivity to light beyond this typical timescale.

Results

Effect of Swimming Velocity: This section focuses on the effect of swimming velocity on the evacuation process. With the velocity controlled and the data obtained as explained in the previous section, plotting the cumulative number of the escaping cells is straightforward. Our study focuses first on a wide door geometry, with $D = 67$ µm $\sim 7 \times a$. The cumulative number of cells escaping

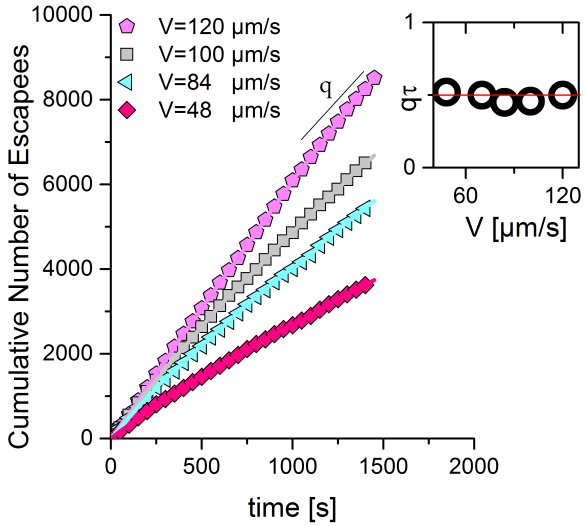

(a) $D = 67$ μm

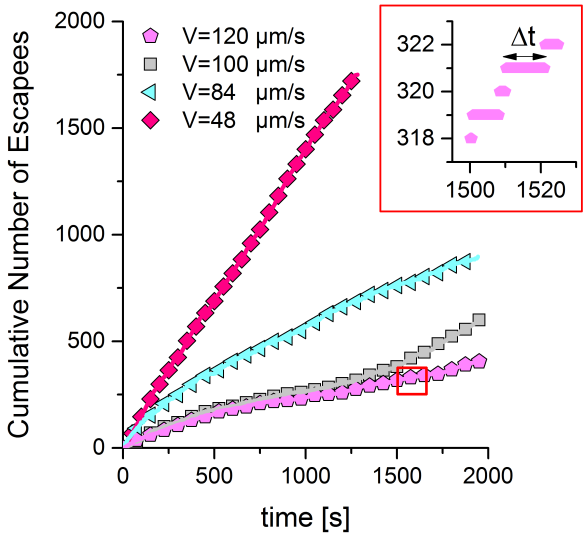

(b) $D = 10$ μm

FIG. 2: Cumulative Number of CR crossing the constriction as a function of time (t) for different swimming velocities. a) Large door size: $D = 67$ μm($\sim 7 \times a$) the flux of particles increases when velocity is increased, the inset shows an equivalence between the flux q and $\tau = \frac{a}{V}$ (Stokes time). b) Small door size $D = 10$ μm($\sim a$) the flux is now decreasing when velocity is increased. Inset: Zoom showing the existence of plateaus *i.e.* longer waiting times Δt.

throughout the experiment plotted in Fig.2a shows a linear trend where a more efficient evacuation occurs with higher swimming velocities. We define the flux q as the number of cells escaping per second. Graphically, it is the slope of linear fits. Fig.2a shows that the flux increases with increasing velocity, meaning the faster the cells swim the more they evacuate. Multiplying q by the Stokes time $\tau = \frac{a}{V}$ (the time that a cell takes to travel a distance equal to its own diameter) gives a value that is independent of velocity, hence the equivalence between τ and q^{-1}. In the same method, when we analyze smaller door size $D = a = 10$ μm, results in Fig.2b show a loss in linearity as V increases with the evacuation being more efficient for slower velocities and q increases with decreasing V.
In order to quantify jamming events, we study statistical distributions of time-lapses Δt (Fig.3b) between two consecutive escaping CRs, known as the survival function:

$$P(t > \Delta t) = \int_{\Delta t}^{\infty} \rho(\Delta t') d\Delta t'.$$

where $\rho(\Delta t')$ is the distribution function of time-lapses. It has been argued [19] that a survival function following a power law decay with an exponent equal to $1 - \alpha$, since $\rho(\Delta t) \sim \Delta t^{-\alpha}$, signifies that the system is susceptible to jam. On the other hand, an uninterrupted flow (i.e flowing state) is represented by a survival function following an exponential decay (*i.e.* an average characteristic time lapse can then be defined).
Visually establishing a linear trend in a logarithmic-scaled histogram is not enough, therefore the method described in [29], known as the Clauset-Shalizi-Newman method (CSN), and its corresponding open source code described in [30] are used to fit tails and extract values of α, the minimum time-lapse above which the trend becomes power law (Δt_{min}) and parameters determining the goodness of fit.
Fig.3a shows the survival function for different swimming velocities for $D = 67$ μm. For all velocities the dominating trend is that of an exponential decay $P(t > \Delta t) \sim \exp(-\frac{\Delta t}{T})$ describing a continuous, uninterrupted evacuation, T being the exponential time. Normalizing time-lapses with τ in inset of Fig.3a, leads to a collapse of all velocities following an exponential decay (solid fit). Fig.3b shows the survival function for different swimming velocities for $D = 10$ μm. We notice as the evacuation velocity increases, the probability to get larger time during which the flux is interrupted increases. In addition, when normalized by τ in inset of Fig.3b, two distinct regimes can be seen. The first, for $\Delta t \leq \tau$, follows an exponential decay, describing a system that is more prone to a flowing state. The second, for $\Delta t > \tau$, the power law trend prevails with a deviation from the exponential trend, with no collapse when time is re-scaled by τ and the

system becomes more susceptible to jamming. Fig.4 shows that the coefficient α decreases with increasing V for $D < 50$ µm, this behavior is found in many systems and is compatible to what might be described as FiS.
On the other hand, the opposite behavior is observed for $D = 50$ µm. Fig.4 shows an increasing value of α with an increasing V, thereby the system is more prone to flow without jamming.

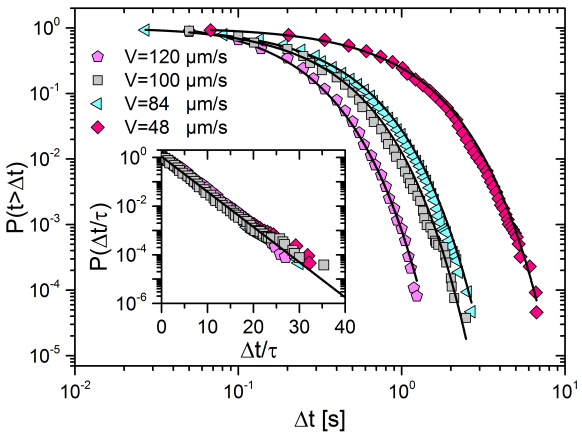

(a) $D = 67$ µm

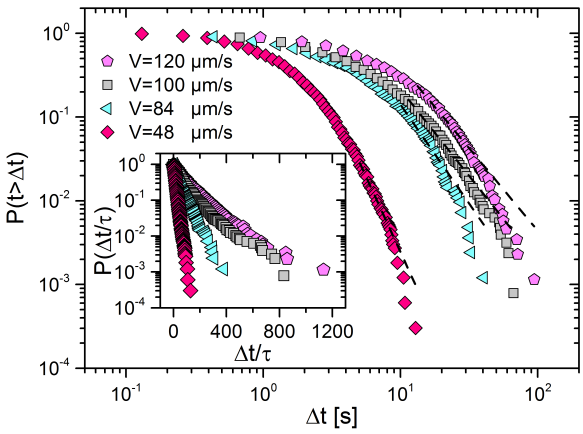

(b) $D = 10$ µm

FIG. 3: Distribution of time lapses between two consecutive escaping CR (survival function) for different swimming velocities. a) $D = 67$ µm. Survival functions are well fitted by an exponential behavior (solid lines). Inset: log-lin representation shows a collapse when re-scaling timescales by τ. b) $D = 10$ µm ($\sim a$). Survival functions show a power law behavior (dashed lines). Inset: log-lin representation shows a deviation from exponential behavior and no collapse when timescales are re-scaled by τ.

Effect of Door Width: In this section we are interested in the effect of door width on the

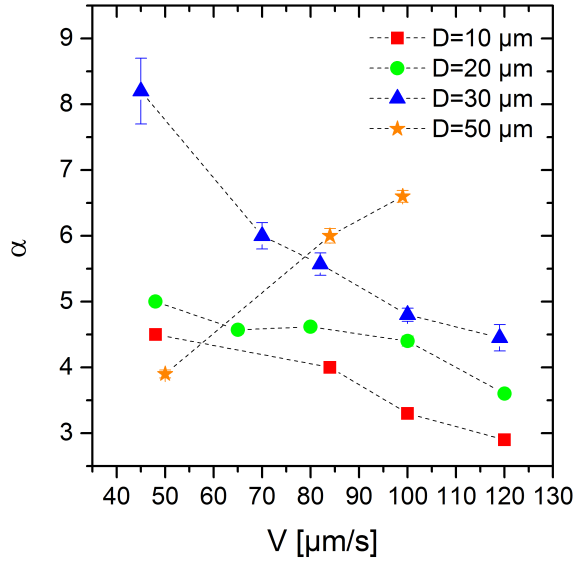

FIG. 4: Power law exponent α of survival functions as function of swimming velocities and different door sizes. For small values of $D(< 50$ µm), α decreases with V, whereas for $D = 50$ µm, α is found to increase with V. Error bars, when not visible, are smaller than symbols.

evacuation process. The analysis is done by fixing the swimming velocity while varying D. In the same procedure detailed in the previous section, we calculate the survival function and extract the coefficient α. Fig.4 shows that at constant V, with increasing D, α increases as well. It means that the evacuation process is less susceptible to jamming, it is also well defined with the previous case of $D = 67$ µm. This observation gives a clue to the presence of a transition zone for 50 µm $\leq D \leq$ 67 µm. We would like to investigate the possibility of empirically calculating the value of a critical diameter D_c, for which we obtain a transition from jamming to flowing state for a given velocity. A similar attempt was recently made for vibrated granular media in [31] where transition is dependent on the vibrating intensity and door size, and in tilted hoppers [32] where the effect of the tilt angle is reported. But first, we need to tackle the problem of finding a Δt above which the system is considered jammed, noted as Δt_c. Such attempts have been made in systems of sheep [33] and horizontal hoppers [34]. In our case we define $\Delta t_c = \Delta t_{min}$ given by the CSN fitting method. For a door size $D = 10$ µm and V varying from 48 µm/s to 120 µm/s, Δt_c varies from 3.15 s to 12 s. We define the avalanche size s as the number of CR that passes through the door between two jamming events, consequently $< s >$

is s averaged over the experiments, for a waiting time Δt, we have a jamming if $\Delta t \geq \Delta t_c$. Having determined the way by which we obtain the avalanche size, we can now investigate the transition from flowing to jamming. Our results [Supplementary Materials] show that $< s >$ grows with D and the behavior can be described empirically by a powerlaw divergence, where $< s >$ increases as D approaches its critical value D_c for which $< s >$ diverges: $< s >= \frac{C}{(D_c - D)^\beta}$ with D_c, C and β being fitting parameters. Interestingly, work done with 3D silo [17] and tilted hoppers with different types of grains [32] shows a similar trend.

Another physical quantity that characterizes the state of the system is the jamming probability. In [35], the authors proposed a probabilistic model describing the behavior of avalanche size s of grains for gravity driven hoppers where jamming is due to arching. Even though we do not observe any arch formation in our experiments, we extend the reasoning to our system. Let us quantify avalanche size s with $\gamma(s)$ which is the probability of finding an avalanche of size s. By definition, an avalanche size consists of one jamming event and s non-jamming events. Therefore, we can write $\gamma(s) = p^s(1-p)$. Here, p is the probability of a CR passing the door without cooperating with its neighbors to form a cluster and jam the door, $J = 1 - p$ is therefore the probability of a CR ability to jam the exit. We assume that p is constant for all CR given the uncorrelated nature of jamming structures. Thus, p is a fitting parameter extracted from experimental data fitted with the above expression of $\gamma(s)$ [Supplementary Materials]. p (and subsequently J) is dependent on both the door size D and the swimming velocity V.

Phase diagram in Fig.5 shows that the predicted values of D_c, extracted from the powerlaw divergence, are in agreement with our experimental results and fall well in the transition zone. In addition, it pin-points the location of phase transition from a dominant power law tail regime for $D < D_c$ where the system is prone to jam, to a domain dominated by an exponential decay for $D \geq D_c$, where the evacuation happens without observable interruption. The color indexing according to J gives an insight to the behavior of our system. Fixing D and increasing V shows an increase in jamming probability, whereas J decreases when fixing V and increasing D until reaching D_c above which $J = 0$.

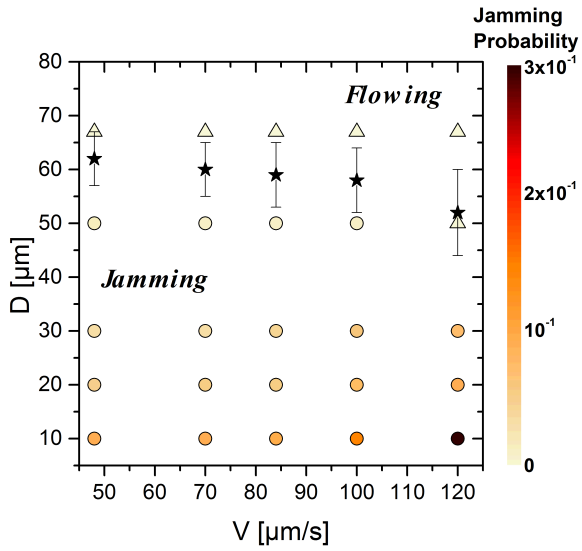

FIG. 5: Active jamming phase $D - V$. For $D < D_c$, a power law behavior of the survival functions indicates jamming ($\circ$). For $D \geq D_c$, a flowing regime is found ($\triangle$) and well described by exponential survival function. Values of D_c ($\star$) are given by $< s >= \frac{C}{(D_c - D)^\beta}$ with error bars being the fitting confidence intervals. Jamming probability follows the color scale.

Conclusion

To conclude, we have developed an experimental approach to study the active jamming of microswimmers at a constriction. We studied the effect of changing the swimming velocity and the opening size, and looked at the results through two different points of view, the first being time-lapse distribution, the other being the avalanche size. We have found that the evacuation process for a given velocity is disturbed for a range of $D < D_c$, whereas for values of $D \geq D_c$ the system does not experience jamming. The approach used in studying granular systems describes well the effect of door size and swimming velocity on the jamming probability, suggesting underlying similarities in jamming issues between both granular and active suspensions. To gain further understanding of the mechanisms at hand in flowing to jamming transition in active suspensions, a thorough investigation of the cell-cell interactions in particular in the dense jammed suspensions would be fruitful.

We thank Romain Mari and Alexandre Nicolas for insightful discussions. We thank the CNRS 80Prime Program for financing this work.

We thank the French-German university program "Living Fluids" (grant CFDA-Q1-14) (M. B.-C.-B., P.P. and S.R.)

[1] E. Matsumura, A. Nakagawa, Y. Tomabechi, S. Ikushiro, T. Sakaki, T. Katayama, K. Yamamoto, H. Kumagai, F. Sato, and H. Minami, Microbial production of novel sulphated alkaloids for drug discovery, Scientific reports **8**, 7980 (2018).

[2] J. J. Milledge and S. Heaven, A review of the harvesting of micro-algae for biofuel production, Reviews in Environmental Science and Bio/Technology **12**, 165 (2013).

[3] A. Nakagawa, E. Matsumura, T. Koyanagi, T. Katayama, N. Kawano, K. Yoshimatsu, K. Yamamoto, H. Kumagai, F. Sato, and H. Minami, Total biosynthesis of opiates by stepwise fermentation using engineered escherichia coli, Nature communications **7**, 10390 (2016).

[4] W. C. DeLoache, Z. N. Russ, L. Narcross, A. M. Gonzales, V. J. Martin, and J. E. Dueber, An enzyme-coupled biosensor enables (s)-reticuline production in yeast from glucose, Nature chemical biology **11**, 465 (2015).

[5] B. K. Hønsvall, D. Altin, and L. J. Robertson, Continuous harvesting of microalgae by new microfluidic technology for particle separation, Bioresource technology **200**, 360 (2016).

[6] A. Karimi, D. Karig, A. Kumar, and A. Ardekani, Interplay of physical mechanisms and biofilm processes: review of microfluidic methods, Lab on a Chip **15**, 23 (2015).

[7] C. R. Cabrera and P. Yager, Continuous concentration of bacteria in a microfluidic flow cell using electrokinetic techniques, Electrophoresis **22**, 355 (2001).

[8] E. Dressaire and A. Sauret, Clogging of microfluidic systems, Soft Matter **13**, 37 (2017).

[9] M. Hassanpourfard, R. Ghosh, T. Thundat, and A. Kumar, Dynamics of bacterial streamers induced clogging in microfluidic devices, Lab on a Chip **16**, 4091 (2016).

[10] H. M. Wyss, D. L. Blair, J. F. Morris, H. A. Stone, and D. A. Weitz, Mechanism for clogging of microchannels, Physical review E **74**, 061402 (2006).

[11] R. Mukhopadhyay, When microfluidic devices go bad (2005).

[12] I. Griffiths, A. Kumar, and P. Stewart, A combined network model for membrane fouling, Journal of colloid and interface science **432**, 10 (2014).

[13] A. Marty, C. Roques, C. Causserand, and P. Bacchin, Formation of bacterial streamers during filtration in microfluidic systems, Biofouling **28**, 551 (2012).

[14] A. Wolff, I. R. Perch-Nielsen, U. Larsen, P. Friis, G. Goranovic, C. R. Poulsen, J. P. Kutter, and P. Telleman, Integrating advanced functionality in a microfabricated high-throughput fluorescent-activated cell sorter, Lab on a Chip **3**, 22 (2003).

[15] A. Lim and R. Bai, Membrane fouling and cleaning in microfiltration of activated sludge wastewater, Journal of membrane science **216**, 279 (2003).

[16] D. Helbing, I. Farkas, and T. Vicsek, Simulating dynamical features of escape panic, Nature **407**, 487 (2000).

[17] I. Zuriguel, A. Garcimartín, D. Maza, L. A. Pugnaloni, and J. M. Pastor, Jamming during the discharge of granular matter from a silo, Phys. Rev. E **71**, 051303 (2005).

[18] M. Souzy, I. Zuriguel, and A. Marin, Transition from clogging to continuous flow in constricted particle suspensions, Phys. Rev. E **101**, 060901(R) (2020).

[19] I. Zuriguel, D. R. Parisi, R. C. Hidalgo, C. Lozano, A. Janda, P. A. Gago, J. P. Peralta, L. M. Ferrer, L. A. Pugnaloni, E. Clément, *et al.*, Clogging transition of many-particle systems flowing through bottlenecks, Scientific reports **4**, 7324 (2014).

[20] E. H. Harris, *The Chlamydomonas sourcebook: introduction to Chlamydomonas and its laboratory use*, Vol. 1 (Academic press, 2009).

[21] M. Polin, I. Tuval, K. Drescher, J. P. Gollub, and R. E. Goldstein, Chlamydomonas swims with two "gears" in a eukaryotic version of run-and-tumble locomotion, Science **325**, 487 (2009).

[22] M. Garcia, S. Berti, P. Peyla, and S. Rafaï, Random walk of a swimmer in a low-reynolds-number medium, Physical Review E **83**, 035301(R) (2011).

[23] X. Garcia, S. Rafaï, and P. Peyla, Light control of the flow of phototactic microswimmer suspensions, Physical review letters **110**, 138106 (2013).

[24] S. Rafai, L. Jibuti, and P. Peyla, Effective viscosity of microswimmer suspensions, Physical Review Letters **104**, 098102 (2010).

[25] The effect of dextran addition on the cell-cell properties of adhesion and lubrification have however not yet been explored.

[26] D. Qin, Y. Xia, and G. M. Whitesides, Soft lithography for micro-and nanoscale patterning, Nature protocols **5**, 491 (2010).

[27] D. B. Allan, T. Caswell, N. C. Keim, and C. M. van der Wel, Trackpy v0.4.1 (2018).

[28] J. C. Crocker and D. G. Grier, Methods of digital video microscopy for colloidal studies, Journal of colloid and interface science **179**, 298 (1996).

[29] A. Clauset, C. R. Shalizi, and M. E. J. Newman, Power-law distributions in empirical data, SIAM Review **51**, 661–703 (2009).

[30] J. Alstott, E. Bullmore, and D. Plenz, powerlaw: A python package for analysis of heavy-tailed distributions, PLoS ONE **9**, e85777 (2014).

[31] R. Caitano, B. V. Guerrero, R. E. R. González, I. Zuriguel, and A. Garcimartín, Characterization of the clogging transition in vibrated granular media, Phys. Rev. Lett. **127**, 148002 (2021).

[32] C. C. Thomas and D. J. Durian, Geometry dependence of the clogging transition in tilted hoppers, Phys. Rev. E **87**, 052201 (2013).

[33] A. Garcimartín, J. M. Pastor, L. M. Ferrer, J. J. Ramos, C. Martín-Gómez, and I. Zuriguel, Flow

and clogging of a sheep herd passing through a bottleneck, Phys. Rev. E **91**, 022808 (2015).

[34] Q.-C. Yu, N. Zheng, and Q.-F. Shi, Clogging of granular materials in a horizontal hopper: Effect of outlet size, hopper angle, and driving velocity, Phys. Rev. E **103**, 052902 (2021).

[35] A. Janda, I. Zuriguel, A. Garcimartín, L. Pugnaloni, and D. Maza, Jamming and critical outlet size in the discharge of a two-dimensional silo, EPL (Europhysics Letters) **84**, 44002 (2008).